

**This is a self-archived version of an original article. This version may differ from the original in pagination and typographic details.**

**Author(s):** Perämäki, Siiri; Tiihonen, Antti; Rajahalme, Joonas; Larsson, Sylva; Lahtinen, Elmeri; Niskanen, Joni; Budhathoki, Roshan; Väisänen, Ari

**Title:** Dry chlorination of spent nickel metal hydride battery waste for water leaching of battery metals and rare earth elements

**Year:** 2022

**Version:** Published version

**Copyright:** © 2022 The Authors. Published by Elsevier Ltd.

**Rights:** CC BY 4.0

**Rights url:** <https://creativecommons.org/licenses/by/4.0/>

**Please cite the original version:**

Perämäki, S., Tiihonen, A., Rajahalme, J., Larsson, S., Lahtinen, E., Niskanen, J., Budhathoki, R., & Väisänen, A. (2022). Dry chlorination of spent nickel metal hydride battery waste for water leaching of battery metals and rare earth elements. *Journal of Environmental Chemical Engineering*, 10(5), Article 108200. <https://doi.org/10.1016/j.jece.2022.108200>



## Dry chlorination of spent nickel metal hydride battery waste for water leaching of battery metals and rare earth elements

Siiri Perämäki, Antti Tiihonen<sup>\*</sup>, Joonas Rajahalme, Sylva Larsson, Elmeri Lahtinen<sup>1</sup>,  
Joni Niskanen, Roshan Budhathoki<sup>2</sup>, Ari Väisänen

Department of Chemistry, Circular Economy, University of Jyväskylä, P.O. Box 35, FI-40014 Jyväskylä, Finland

### ARTICLE INFO

Editor: Fumitake Takahashi

#### Keywords:

NiMH  
Battery  
Dry chlorination  
Leaching  
Rare earth element

### ABSTRACT

An efficient leaching process was developed for nickel, cobalt, and the rare earth elements (REEs) from spent nickel metal hydride (NiMH) battery waste. The process involves dry chlorination with ammonium chloride in low temperature to produce water-soluble chlorinated compounds, followed by simple water leaching. The factors affecting the conversion and solubilization were studied, including the amount of ammonium chloride, residence time and temperature in dry chlorination, and solid to liquid ratio, time and temperature in water leaching. As a result, the dry chlorination process was found to produce ammonium and chloride containing products, depending on the temperature of the process: ammonium metal chlorides were produced in temperatures of 250–300 °C, while increasing the temperature to 350 °C resulted in formation of metal chlorides. Overall, highest metal recoveries were achieved during 60 min residence time at a temperature of 350 °C, where ammonium is no longer present and ammonium metal chlorides and metal chlorides have formed. Water leaching was found to proceed rapidly, especially for REEs, and yields of 87% for Ni, 98% for Co, 94% for Ce, and 96% for La were attained during 60 min of leaching in room temperature. This study introduces a process, which is considered as an environmentally more benign alternative to traditional mineral acid leaching, resulting in high metal leaching efficiencies with neutral leachates, requiring no chemical-intensive neutralization steps in the following processing.

### 1. Introduction

Critical raw materials, first defined and listed by the European Commission in 2010 [1], have since gathered much of the attention of the scientific community and related industries. The list consists of materials having a high supply risk and high economic importance to the European Union, with 30 materials as of 2020 [2]. The list of critical materials includes many of the materials used in nickel-metal hydride (NiMH) batteries, such as cobalt and rare earth elements (REEs). Furthermore, nickel is included in the list of candidate materials, ones that might be classified as critical in future assessments depending on their respective supply risks. For this reason, the recycling of NiMH batteries and the recovery of valuable metals from them has been of great interest in the past decade.

NiMH batteries were introduced to the consumer market at the end of the 1980s and came to replace the structurally similar but more

environmentally hazardous nickel-cadmium batteries in many applications [3]. Most notably they have found use in hybrid electric vehicles (HEVs), and with a significant 50% growth rate in new registered HEVs in the EU between 2018 and 2019, the annual NiMH battery waste volume is estimated to reach 33 600 tonnes in 2030 [4]. The major components of a NiMH battery are the positive and negative electrodes, casing materials, electrolyte and separator(s) [5]. The cathode of a NiMH battery consists of nickel hydroxide while the most common anode material is an intermetallic compound AB<sub>5</sub>, where A is mischmetal – a rare-earth mixture of lanthanum, cerium, praseodymium and neodymium (Ln) – and B is nickel, cobalt, manganese and aluminium. The exact composition of NiMH batteries varies somewhat depending on their application and cell type, e.g. smaller portable cells may contain 36–42% of Ni, 3–4% of Co and 8–10% of mischmetal by weight [3,6]. For a plug-in HEV battery pack, these percentages are slightly lower due to the added structural components and casing

<sup>\*</sup> Corresponding author.

E-mail address: [antti.j.tiihonen@jyu.fi](mailto:antti.j.tiihonen@jyu.fi) (A. Tiihonen).

<sup>1</sup> Present address: Weeefiner LTD, Survontie 9B, FI-40500, Jyväskylä

<sup>2</sup> Present address: Metso Outotec LTD, P.O. Box 1220, FI-0010, Helsinki

materials, such as steel and plastics.

Existing recycling processes for NiMH batteries are mainly ones that utilize a mechanical and/or a thermal pretreatment, and a subsequent chemical treatment. Pyrometallurgical processes are applied mainly for the recovery of nickel and other base metals, since REEs are lost in the slag in these processes [3]. As for the hydrometallurgical processes able at recovering both REEs and battery metals, acid leaching with mineral acids appears to be the most commonplace practice [3,5,7–11]. Other leaching processes have also gained attention in recent years, including bioleaching [12,13], ionic liquids [14,15], and subcritical water [16], with all of them aiming at environmentally more sound metal recovery. Alternative recovery processes for spent NiMH batteries with emphasis on environmental aspects are indeed needed in the future.

Dry chlorination or solid-state chlorination comprises a variety of methods with the aim of producing easily soluble metal chlorides for further processing. Chlorination has been studied since the 1950s in the extraction of REEs and other metals from various minerals [17], and has gained interest in the recent years for use in the recovery of valuable metals from waste streams such as neodymium magnet sludge [18], spent neodymium magnets [19,20], chemical sorbents [21], and NiMH batteries [22]. Traditionally such waste materials would be digested using mineral acids [23], which are not only expensive themselves, but necessitate the eventual neutralization of the acidic leaching medium producing saline waste waters which in turn need to be disposed of, adding to the cost of the process. Dry chlorination removes the need to use mineral acids as the produced metal chlorides are readily dissolved in water, making further processing easier. The chlorination of metals can be achieved with roasting the materials at a sufficiently high temperature in the presence of various chlorination agents, including chlorine gas ( $\text{Cl}_2$ ) [17,24], carbon tetrachloride gas ( $\text{CCl}_4$ ) [22], calcium chloride ( $\text{CaCl}_2$ ) [25], sodium chloride ( $\text{NaCl}$ ) [25], magnesium chloride ( $\text{MgCl}_2$ ) [25], iron(III)chloride ( $\text{FeCl}_3$ ) [25], iron(II)chloride ( $\text{FeCl}_2$ ) [18] and ammonium chloride ( $\text{NH}_4\text{Cl}$ ) [19,20,24,26]. The use of  $\text{NH}_4\text{Cl}$  offers many advantages over the other chlorination agents by being easier and safer to handle than toxic  $\text{Cl}_2$  and  $\text{CCl}_4$  gases, while introducing no alien elements into the process unlike the other salts. Unreacted  $\text{NH}_4\text{Cl}$  can also be readily recovered from the gas stream leaving the reactor with a scrubber, and the obtained by-product of  $\text{NH}_3$  solution used for example as a fertilizer [20]. To our knowledge, dry chlorination of NiMH batteries using specifically  $\text{NH}_4\text{Cl}$  as the active agent has not been proposed and evaluated, only the comprehensive works of Ma et al. [26] coming very close to the subject at hand albeit with Li-Ion, not NiMH, batteries and similarly Kuzuya et al. [22] with NiMH material but with  $\text{CCl}_4$  as the agent.

In the present work, a method for the dry chlorination of spent NiMH battery waste was developed and investigated using  $\text{NH}_4\text{Cl}$  specifically as the chlorination agent. Dry chlorination was followed by water leaching of the formed chlorination products to leach Ni, Co, and REEs into solution. This enables the production of a neutral leachate, removing the chemical-intensive step of neutralization in the following processing stages. For the dry chlorination process, several parameters were studied in regards to the efficiency of the process, e.g. NiMH: $\text{NH}_4\text{Cl}$  mass ratio, time, and temperature. To study the reaction products formed in the dry chlorination process, X-ray diffraction (XRD), infrared (IR) -spectrometry, scanning electron microscopy (SEM), and water leaching followed by elemental analysis were performed for the dry chlorination products. After finding the optimal dry chlorination parameters, an investigation of water leaching parameters was finally performed. This study introduces an alternative process to traditional mineral acid leaching of spent NiMH battery waste: dry chlorination in low temperature followed by simple water leaching, resulting in high yields for battery metals Ni and Co, as well as the REEs.

## 2. Material and methods

### 2.1. The spent NiMH battery waste and characterization

Crushed electrode materials from spent NiMH batteries were received from a Finnish recycling company, Akkuser LTD. The spent NiMH battery waste (NiMH material) was sieved to a particle size of  $< 500 \mu\text{m}$ , which was used throughout the study. Elemental composition of the NiMH material was analyzed using ICP-OES (Avio 500, PerkinElmer, U.S.), after microwave assisted digestion (Mars 6 iWave, CEM, U.S.) in aqua regia. Four replicate samples were digested and analyzed for 67 elements (see Table S1) after dilution in 5% nitric acid (67%, puriss p.a., Sigma Aldrich). Ultrapure water was used in all experiments (PureLab Ultra, Elga, U.K.). Concentrations of C, H, and N were determined from solid samples using elemental analyzer (Vario EL III, Elementar Analysensysteme GmbH, Germany).

Surface morphology of the samples was imaged with SEM (EVO-50XVP, ZEISS, Germany) and analyzed with energy-dispersive x-ray fluorescence (EDXRF) (Quantax400 EDS, Bruker Corporation, U.S.). The sample was attached onto carbon tape and back-scattering detector was utilized for imaging. IR measurements were performed using a FT-IR spectrometer (Nicolet iS50, Thermo Fisher Scientific, U.S.) in an ATR mode. X-ray powder diffraction (XRD) analyses were conducted on a powder diffractometer (X'Pert Pro Alpha1 MPD, Malvern PANalytical, U.K.) using a fixed-anode Cu tube operating at 45 kV and 40 mA ( $\text{Cu K}\alpha_1 \lambda = 1.5406 \text{ \AA}$ ). Incident beam was Ni-filtered and a programmable divergence slit (PDS) was installed to control sample irradiation with a fixed area of  $10 \times 10 \text{ mm}$  in a circular 16 mm stainless steel sample cavity over a  $2\theta$ -range of  $5 - 85^\circ$  with  $0.017^\circ$  and 160 s step size and counting time, respectively. Diffracted intensities were recorded with an X'Celerator detector and analyzed using PANalytical HighScore Plus (v. 4.9) and the latest PDF4+ reference database. Data corrections applied in software were stripping of  $\text{K}\alpha_2$  wavelength and PDS conversion from automatic to fixed ( $0.50^\circ$ ). Diffraction data over very low ( $5-15^\circ$ ) or very high angle range ( $65-85^\circ$ ) was not included in the graphical presentation due to low peak intensities close or below the baseline but was included in the peak profile refinement and subsequent database search.

### 2.2. Dry chlorination

Ammonium chloride ( $\text{NH}_4\text{Cl}$ ) with a purity of  $> 99\%$  supplied by Aldrich, was ground in a ball mill (S1000, Retsch, Germany) for 15 min. The NiMH material was ground in a mortar for 5 min, and then combined with the ground  $\text{NH}_4\text{Cl}$  in a wt.-ratio of 1:1.65, respectively. The mixture was mixed thoroughly in a mortar for 15 min. Fresh NiMH: $\text{NH}_4\text{Cl}$  -mixture was prepared on a daily basis.

A 0.5 g sample of the NiMH: $\text{NH}_4\text{Cl}$  -mixture was weighed into a tared porcelain crucible, which was covered with a lid and placed in a muffle furnace (CWF1300, Carbolite, U.K.) at room temperature of  $21^\circ\text{C}$ . The furnace was ramped to 250, 300 or  $350^\circ\text{C}$  at a rate of  $10^\circ\text{C}$  per min, and then held for 30–120 min before removal from the furnace. The crucible was placed into a desiccator for 30 min for cooling, after which it was weighed. Two replicate samples were prepared for each dry chlorination condition.

### 2.3. Water leaching

A 0.25 g sample of the roasted material was weighed into a 50 ml polypropylene vessel, into which 25 ml of ultrapure water and a magnetic stirrer bar was added. The leaching was done by placing the vessel on a magnetic stirrer plate at room temperature ( $21^\circ\text{C}$ ), or on a water bath stabilized at a temperature of  $60^\circ\text{C} (\pm 3^\circ\text{C})$  for 30 or 60 min. A 5 ml sample aliquot was taken immediately after mixing, or after 30 or 60 min of leaching, and filtered with a no. 42 Whatman filter paper. The sample was diluted in 5% nitric acid for elemental analysis using ICP-OES. Three replicate samples were prepared for each leaching condition.

### 3. Results and discussion

#### 3.1. Characterization of the spent NiMH battery waste

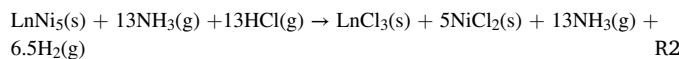
From the elemental analysis of the NiMH material, Ni and Co were determined as the major components at 40 and 7.6 wt%, respectively, as presented in Table 1. Nickel is present in the sample as typical cathode and anode compounds found in NiMH batteries: Ni(OH)<sub>2</sub> (phase I) and LnNi<sub>5</sub> type compounds LnNi<sub>4+x</sub>(Al,Mn,Co...)<sub>1-x</sub> (phase II), which were identified in the XRD analysis presented in Fig. 1A. Cobalt is also found in compound LiCoO<sub>2</sub> (phase III), indicating that the starting material has some Li-ion battery material mixed with the NiMH material. This is supported by the detection of graphite (phase IV) in the sample, also a Li-ion battery material. Since the NiMH material used in the study was obtained from a recycling company also treating Li-ion batteries, some impurities in the material are to be expected. The total REE content in the material is approximately 16 wt%, with lanthanum as the most abundant REE at 8.7 wt%. Other major components are carbon, manganese, and potassium, at 5.1, 2.2, and 1.9 wt%, respectively. Low concentrations of other elements were found in the NiMH material as well, consisting of 7.6 wt% of the total sample weight (detailed elemental concentrations are presented in Table S1). Elemental analysis resulted in approximately 80% of the sample weight, while the rest of the sample consist of elements which were not analyzed, such as oxygen. The different components of the NiMH batteries can be seen in the SEM image of the NiMH material in Fig. 1B. as heterogeneity in size, form, and charging (i.e. color) of the particles.

#### 3.2. Dry chlorination and mass ratio of NiMH:NH<sub>4</sub>Cl

During dry chlorination, NH<sub>4</sub>Cl is decomposed at 338 °C [27] via R1 to NH<sub>3</sub> and HCl, which will in turn react with the metals present in the NiMH material. However, the decomposition of NH<sub>4</sub>Cl is an equilibrium reaction steered by partial pressures of NH<sub>3</sub> and HCl, beginning already at a temperature of 220 °C, but with lower reaction rate [28]. In fact, the use of lower temperatures has resulted in higher REE yields in the dry chlorination of fluorescent lamps and neodymium magnets, when compared to temperatures higher than 338 °C [28,29]. This can be explained by the different reaction rates of the decomposition and chlorination reactions: if the decomposition of NH<sub>4</sub>Cl proceeds too quickly, the produced gases are displaced from the reactor before the chlorination reaction has happened [20]. According to the factors stated above and our initial dry chlorination experiments, a temperature of 300 °C with a residence time of 60 min was chosen for the for evaluation of a suitable amount of NH<sub>4</sub>Cl to the NiMH material. A slow ramp time of 10 °C per minute was also employed to prevent premature loss of gaseous decomposition products NH<sub>3</sub> and HCl from the reaction vessels.

An appropriate NiMH:NH<sub>4</sub>Cl –ratio was assessed to ensure the efficiency of the dry chlorination process, where there is enough NH<sub>4</sub>Cl for completion of the dry chlorination reactions, but not in large excess. Since the main component in the NiMH material is LnNi<sub>5</sub>, the amount of NH<sub>4</sub>Cl needed in the dry chlorination can be assessed from the chlorination reaction R2. To one mole of LnNi<sub>5</sub>, 13 moles of NH<sub>4</sub>Cl is required, which results in a theoretical minimum mass of 1.6 fold of NH<sub>4</sub>Cl compared to the mass of the NiMH material. However, there are other compounds in the NiMH material that react with NH<sub>4</sub>Cl as well (e.g. reaction R3), and other possible reactions that can occur during the dry chlorination (see Section 3.3). Hence, the required mass of NH<sub>4</sub>Cl was experimentally studied at 1.0, 1.5 and 2.0 fold compared to the mass of

the NiMH material. The dry chlorination process was followed by water leaching using 60 °C temperature with 30 min leaching time, which were found to be sufficient conditions for water leaching during preliminary experiments. Since the sample at hand was a real-life material obtained from a company and separate tests using synthetic samples were not conducted to further elucidate the reaction mechanisms and validate exact reaction pathways, separate future studies are conducted. Furthermore, the reactions presented here and following in Sections 3.4 and 3.5 are only regarded as a frame of reference for these initial leaching experiments and could be elucidated further.



The use of different amounts of NH<sub>4</sub>Cl was found to have different effects on the leaching efficiencies of Ni and Co compared to the REEs, La and Ce, as seen in Fig. 2. The mass ratio of NiMH:NH<sub>4</sub>Cl has a clear effect on the leaching efficiency of Ni and Co when 1:1 and 1:1.5 ratios are compared, with the sub-stoichiometric ratio 1:1 resulting in lower leaching efficiencies. This was to be expected, as the ratio 1:1 is estimated as substoichiometric according to R2. When ratios 1:1.5 and 1:2 are considered, very similar leaching efficiencies of Ni and Co are attained, and increase in the amount of NH<sub>4</sub>Cl appears to be unnecessary. The effect of NiMH:NH<sub>4</sub>Cl ratio on the leaching efficiency of REEs La and Ce is minor, with no clear difference in their leaching efficiencies even with 1:1 ratio. The observed difference in behaviour of Ni and Co compared to the REEs indicates that soluble REE chlorination products are more readily formed than Ni and Co chlorination products. Since no significant differences were observed between the 1.5 and 2.0 fold amounts of NH<sub>4</sub>Cl, indicating enough NH<sub>4</sub>Cl in both mixtures, the amount of NH<sub>4</sub>Cl was chosen as 1.65 fold to the mass of the NiMH material in subsequent experiments, slightly above the stoichiometric amount according to R2. The ratio of 1:1.65 should not therefore be considered as completely optimized with regard to e.g. chemical consumption, but it serves as a valid first estimate parameter value in the testing, and was carried unchanged throughout the rest of studies. Furthermore, inadequate reaction conditions regarding downstream reactions in or outside the reaction vessel or deterioration of oven materials from evolving reactive gases were not taken into account, but should be considered in the future, especially when up-scaling the process and choosing kiln and gas scrubber materials.

#### 3.3. Dry chlorination temperature and residence time

##### 3.3.1. Temperature

The effect of temperature on dry chlorination process was first studied using temperatures of 250, 300, and 350 °C and a residence time of 120 min. The mass loss of the NiMH:NH<sub>4</sub>Cl mixture was used to evaluate the vaporization of volatile compounds (e.g. NH<sub>3</sub>, H<sub>2</sub>, H<sub>2</sub>O, O<sub>2</sub>) produced in the chlorination reactions. As expected, temperature had a significant effect on the loss of volatile compounds, as seen in Fig. S1: at the lowest temperature of 250 °C, a total mass loss of 12% was observed after residence time of 120 min, and by using higher roasting temperatures of 300 and 350 °C, higher mass losses of 25% and 38% were observed, respectively. Significant changes in the appearance of the NiMH:NH<sub>4</sub>Cl mixture were also evident after dry chlorination at

**Table 1**  
Concentrations (wt%) of elements in the NiMH material.

Battery metals and other elements (wt%)						Rare earth elements (wt%)					
Ni	Co	C	Mn	K	Other	La	Ce	Pr	Nd	Sm	Total REE
39.8	7.59	5.07	2.24	1.88	7.60	8.65	4.74	0.72	1.90	0.21	16.23



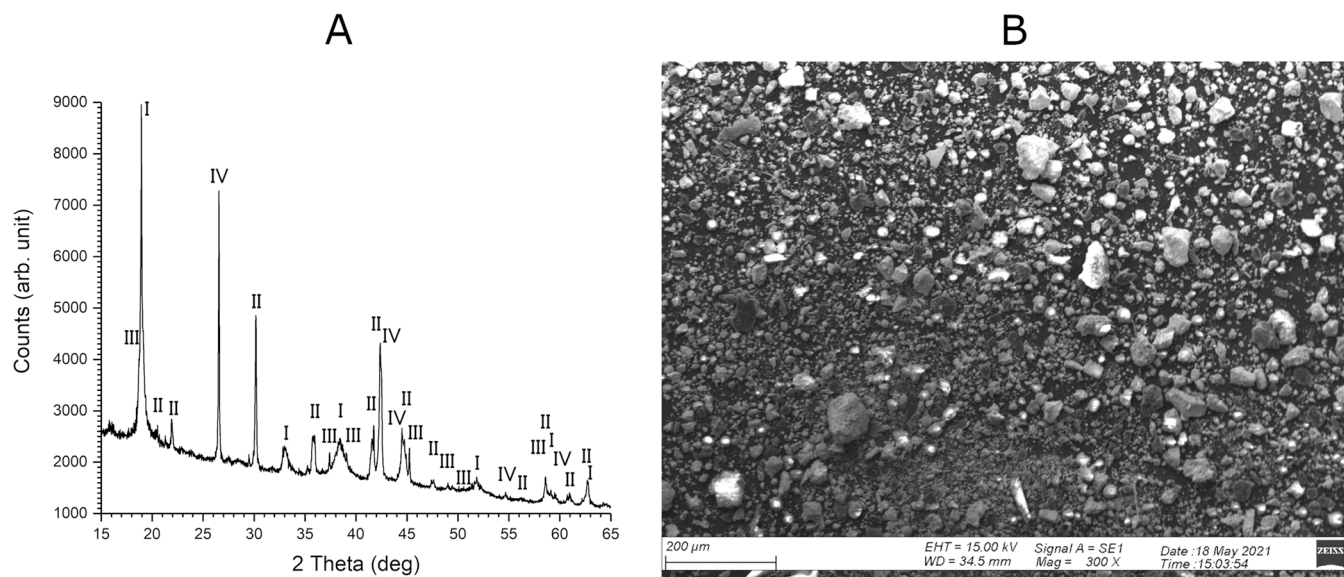


Fig. 1. A) XRD pattern of the NiMH material. Major phases: Ni(OH)<sub>2</sub> (I), LnNi<sub>5</sub> (Ln = Ce, La, Nd, Pr) (II), LiCoO<sub>2</sub> (III) and C (IV). B) SEM image of the NiMH material.

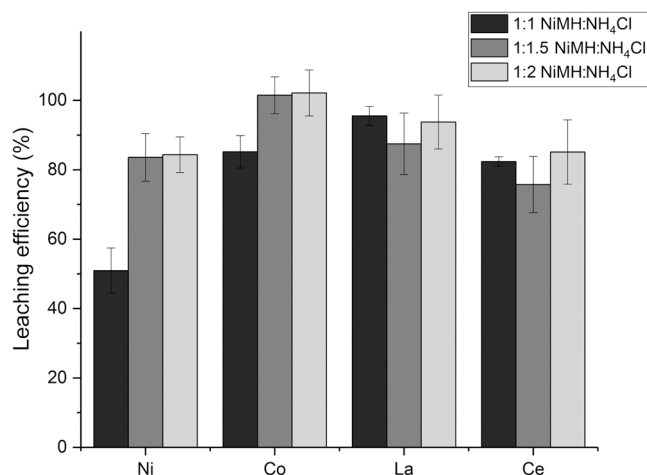


Fig. 2. Effect of mass ratio of NiMH:NH<sub>4</sub>Cl (1:1, 1:1.5, 1:2) on the leaching efficiency (%) of Ni, Co, La, Ce. Dry chlorination conditions: temperature = 300 °C, residence time = 60 min.

different temperatures, as seen in SEM images of the dry chlorinated residues in Fig. S2 A-C. As the temperature of the dry chlorination process is increased, a more crystalline appearance is observed in the samples, indicating formation of different crystal structures in the formed reaction products depending on the dry chlorination temperature.

IR spectra of the NiMH:NH<sub>4</sub>Cl mixtures shown in Fig. S3 A-E for different dry chlorination temperatures also displays significant changes in the residues formed. NH<sub>4</sub>Cl is still present in the dry chlorination residues at 250 or 300 °C after 120 min, and is absent only when temperature of 350 °C is used, which was to be expected regarding the decomposition temperature of 338 °C for NH<sub>4</sub>Cl. Nickel(II) hydroxide is observed at wavenumber 3630 cm<sup>-1</sup> in the original mixture, but is not found in the spectra of the dry chlorinated residues in any of the used temperatures, indicating that it is easily reacted during the dry chlorination process. When a temperature of 300 °C is used, ammonium nickel (II) chloride dihydrate is observed in the residue, but in the highest temperature of 350 °C, the ammonium is not present anymore and nickel(II) chloride dihydrate is obtained. It should be noted that the IR spectra library found correspondence to ammonium copper(II) chloride

dihydrate and copper(II) chloride dihydrate, but since the sample contains very low concentrations of copper, this was assumed to be the corresponding nickel compounds, with very similar chemical behaviour to copper. This data clearly demonstrates that the chlorination reactions are dependent on the dry chlorination temperature, and that different reaction products are present in the residues treated at different temperatures: ammonium metal chlorides in 300 °C and metal chlorides at 350 °C.

### 3.3.2. Residence time

To gain further information on the formation of different compounds during the dry chlorination process, the effect of temperature and residence time was further studied using residence times of 30, 60, 90, 120 min in temperatures of 250, 300 and 350 °C. The samples were analyzed by XRD to identify the produced compounds, and further water leached to evaluate the effect on solubility of Ni, Co, and the REEs. As seen from the XRD patterns in Fig. 3 A-C, the formation of ammonium containing metal chlorides is present in all temperatures, but predominantly in 250 °C and 300 °C. The incomplete decomposition of NH<sub>4</sub>Cl (phase S) can also be seen in these temperatures, verifying the findings of the IR measurements. Metal chlorides are observed to be formed only in the highest temperature of 350 °C after 60 min of residence time.

A closer investigation of the phases present in 250 °C shows the evolution of ammonium Ni/Co chlorides, NH<sub>4</sub>NiCl<sub>3</sub> (phase A) and (NH<sub>4</sub>)<sub>3</sub>CoCl<sub>5</sub> (phase B), from 60 min and onwards. The appearance of peaks originating from ammonium REE chlorides, (NH<sub>4</sub>)<sub>2</sub>LnCl<sub>5</sub> (phase C), begins at 90 min mark, which also coincides with the solubility maxima of La and Ce in the water leaching, presented in Fig. 4A for 250 °C. This points to good solubility of the observed ammonium REE chlorides at 90 min residence time, with 79% and 74% water leaching efficiency for La and Ce, respectively. In the same conditions, only 32% of Ni and 59% of Co were found with water leaching, indicating lower solubility of the observed ammonium Ni/Co chlorides. Additional increase in the residence time from 90 min onwards has minor effect on the leaching efficiencies of the studied metals.

In 300 °C, the evolution of products is faster with NH<sub>4</sub>NiCl<sub>3</sub> appearing already in 30 min whereas (NH<sub>4</sub>)<sub>3</sub>CoCl<sub>5</sub> has formed in 60 min and will eventually disappear after 90 min, indicating an intermediate product. Present after 60 min is also phase M that is generally not well resolved and contains compounds that were not unambiguously interpreted, chemically corresponding most closely to NH<sub>4</sub>LnCl<sub>4</sub>·3H<sub>2</sub>O and analogues to phase C (see SI for further details). After 60 min residence

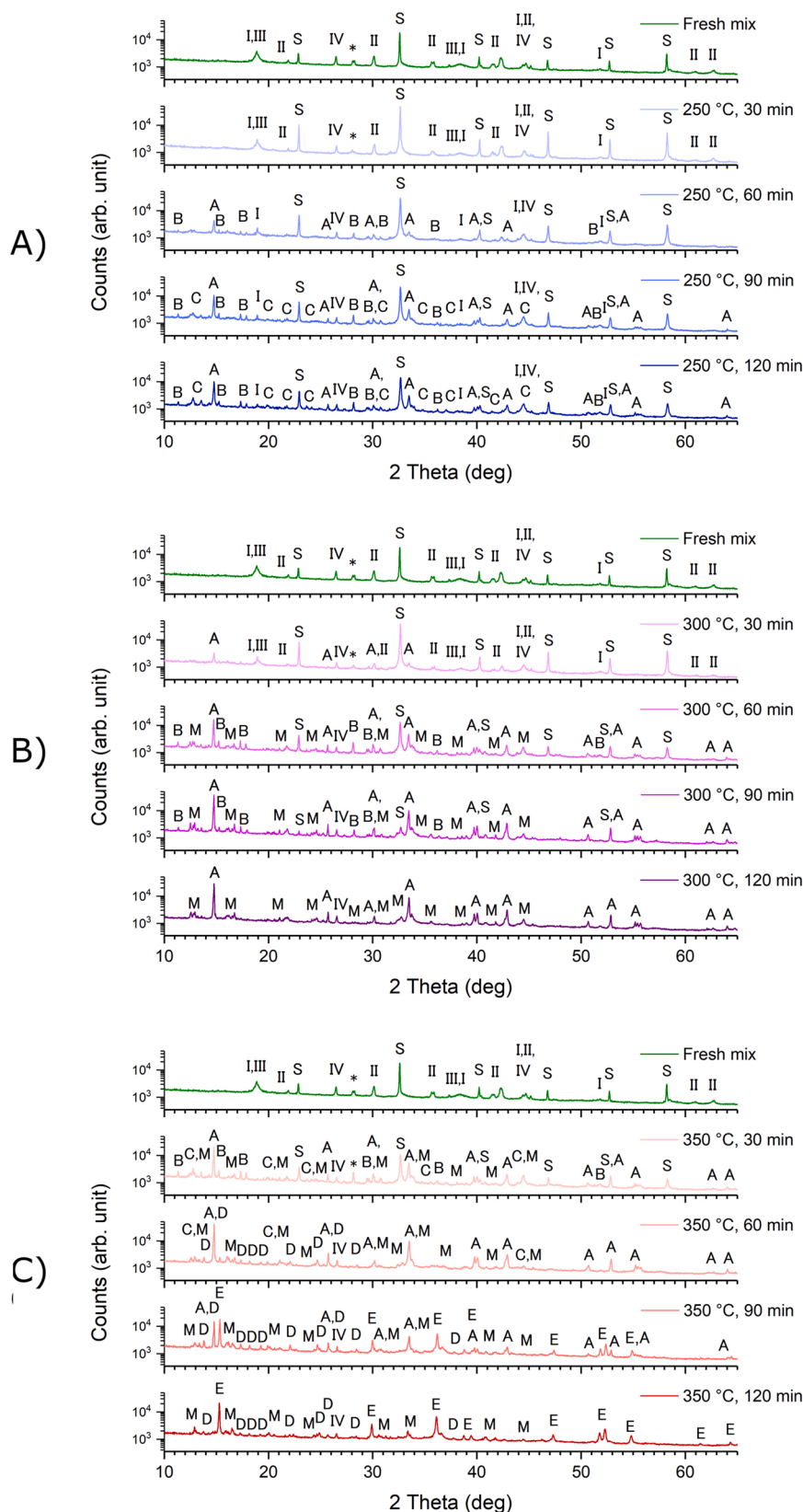


**Fig. 3.** A-C. Powder diffraction patterns of NiMH:NH<sub>4</sub>Cl mixtures treated in A) 250 °C, B) 300 °C, and C) 350 °C with different residence times (30, 60, 90 and 120 min) in comparison to the fresh mixture of 1:1.65 NiMH:NH<sub>4</sub>Cl. Peak \* is undetermined and not found in the un-mixed NiMH material. Major phases: NH<sub>4</sub>Cl (S), Ni(OH)<sub>2</sub> (I), LnNi<sub>5</sub> (Ln = Ce, La, Nd, Pr) (II), LiCoO<sub>2</sub> (III), C/graphite (IV), NH<sub>4</sub>NiCl<sub>3</sub> (A), (NH<sub>4</sub>)<sub>3</sub>CoCl<sub>5</sub> (B), (NH<sub>4</sub>)<sub>2</sub>LnCl<sub>5</sub> (C), LnCl<sub>3</sub>·6H<sub>2</sub>O (D), CoCl<sub>2</sub> (E) and NH<sub>4</sub>LnCl<sub>4</sub>·3H<sub>2</sub>O (M, see SI).

time, high leaching efficiencies of 98–100% were achieved for both La and Ce (Fig. 4B), indicating that the observed REE containing mixed phase M is highly soluble, similar to (NH<sub>4</sub>)<sub>2</sub>LnCl<sub>5</sub> (phase C). Leaching efficiencies of Ni and Co are also substantially better compared to those

in 250 °C, but complete leaching is yet not achieved as the highest leaching efficiencies remain at 78% for Ni and 92% for Co with 90 min residence time.

In 350 °C, ammonium metal chlorides (NH<sub>4</sub>NiCl<sub>3</sub>, (NH<sub>4</sub>)<sub>3</sub>CoCl<sub>5</sub>,

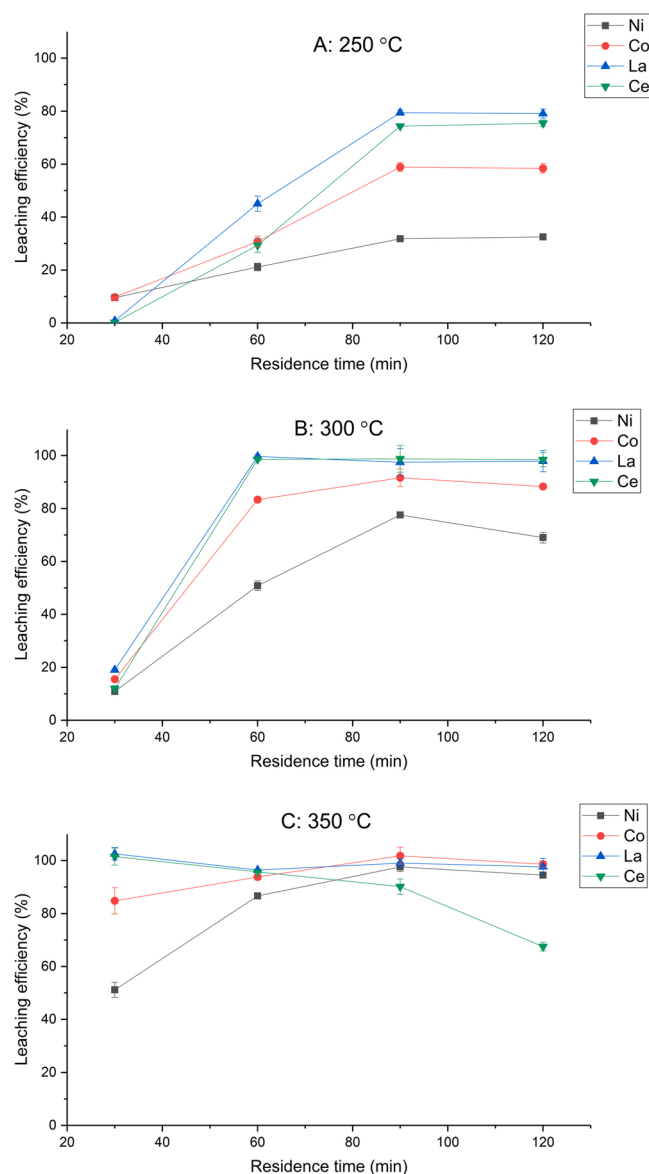


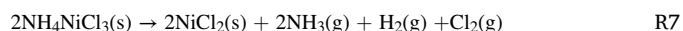
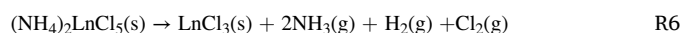
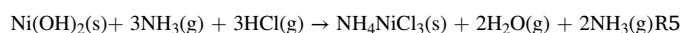
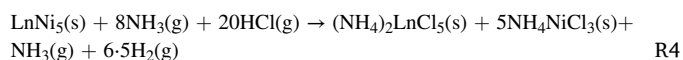
**Fig. 4.** A-C. Effect of dry chlorination residence time (min) on water leaching efficiency (%) of Ni, Co, La, and Ce at temperatures of A) 250 °C, B) 300 °C, and C) 350 °C.

( $(\text{NH}_4)_2\text{LnCl}_5$  and phase M) are detected already at the 30 min mark, followed by the evolution of REE chlorides,  $\text{LnCl}_3 \cdot 6\text{H}_2\text{O}$  (phase D), starting from 60 min onwards. Here,  $\text{NH}_4\text{Cl}$ ,  $(\text{NH}_4)_3\text{CoCl}_5$ , and most of  $(\text{NH}_4)_2\text{LnCl}_5$  have already disappeared.  $(\text{NH}_4)_2\text{LnCl}_5$  is gone when 90 min is reached and  $\text{NH}_4\text{NiCl}_3$  is on the decline, but a final new product  $\text{CoCl}_2$  (phase E) is now present. This marks the solubility maxima of both Ni and Co with 98% and 102% water leaching efficiencies, respectively, as seen in Fig. 4 C, indicating that chloride formation is needed to reach total dissolution of Ni and Co. It should be noted that  $\text{NiCl}_2$  was not detected separately, but as an isostructural compound it can be included in the interpretation of the detected  $\text{CoCl}_2$  pattern, see SI for further discussion. In the concluding 120 min mark,  $\text{NH}_4\text{NiCl}_3$  has disappeared, and  $\text{CoCl}_2$  dominates the pattern next to  $\text{LnCl}_3 \cdot 6\text{H}_2\text{O}$  and phase M. In comparison to Ni and Co, the leaching efficiency of Ce and other REEs (excluding La) decreases as the residence time is increased, which was not observed in the lower temperatures. Since REE chlorides have high solubilities (96–100 g per 100 g of water for  $\text{CeCl}_3$ ,  $\text{NdCl}_3$  and  $\text{PrCl}_3$  [27]), the formation of chlorides with increasing residence time cannot explain the decrease in leaching

efficiency observed for other REEs than La. Instead, the lower leaching efficiency observed for REEs could be caused by the formation of some insoluble reaction products, e.g. REE oxides and oxychlorides [22], which would remain undetected in XRD due to their presumably low concentrations and the complex nature of the sample material.

### 3.4. Dry chlorination reactions

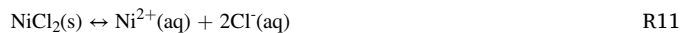
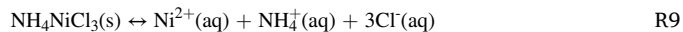
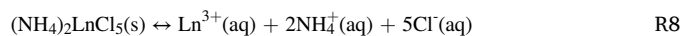
Based on the findings from the IR and XRD measurements as well as the water leaching experiments, the dry chlorination process appears to proceed via ammonium metal chloride intermediates to metal chlorides. The proposed reactions during dry chlorination using  $\text{NH}_4\text{Cl}$  as the chlorination reactant are the formation of ammonium metal chloride intermediates (R4 and R5) followed by their decomposition and formation of metal chlorides in reactions R6 and R7:



A similar finding was made by Ma et al. [26] when studying dry chlorination of spent lithium-ion battery cathode material with  $\text{NH}_4\text{Cl}$ : formation of ammonium metal chlorides ( $\text{NH}_4\text{NiCl}_3$ ,  $\text{NH}_4\text{CoCl}_3$ ,  $\text{MnCl}_2 \cdot \text{NH}_3$ ) was reported at a temperature of 250 °C, and as the temperature was increased, the reaction products were stabilized as metal chlorides ( $\text{NiCl}_2$ ,  $\text{CoCl}_2$ ,  $\text{CoCl}_2 \cdot 2\text{H}_2\text{O}$ ,  $\text{MnCl}_2$  and  $\text{LiCl} \cdot \text{H}_2\text{O}$ ) at temperatures of 350 and 400 °C. Interestingly, when  $\text{CCl}_4$  was used for chlorination of NiMH battery waste by Kuzuya et al. [22], a temperature of 500 °C was required for most of the nickel to be chlorinated. At a lower chlorination temperature of 400 °C, the authors reported REE chlorides and insoluble nickel alloy formation, as well as minor amounts of REE oxychlorides.

### 3.5. Water leaching

After finding most suitable conditions for the dry chlorination process, the effects of S:L-ratio, time, and temperature on the water leaching process were finally studied. The dry chlorination for the water leaching experiments was done using overall optimal 60 min residence time and temperature of 350 °C. The water leachate was sampled immediately after mixing of the sample and water ( $t = 0$ ), and at 30- and 60-min time intervals. Four S:L-ratios were examined in room temperature (21 °C), and at elevated temperature of 60 °C. The formed dry chlorination products are dissolved in water according to reactions R8–R11:



For Ni and Co, longer leaching time increases the yields especially in room temperature, but a significant amount of > 50% is leached with all S:L-ratios even immediately after mixing, as seen in Fig. 5 A-D. A more dilute S:L-ratio seems to be more efficient in leaching of Ni and Co in room temperature, however, at elevated temperatures the differences between different S:L-ratios are smaller. In the case of La and Ce, the effect of leaching time and S:L-ratio was minor (Fig. 6 A-D), and S:L-ratio of 1:100 results in 90–94% leaching efficiencies immediately after mixing in both temperatures. The dissolution reaction can be considered very fast for REEs, and elevated temperature is not needed even when the leaching time is as short as 30 min. No clear trend is observed for

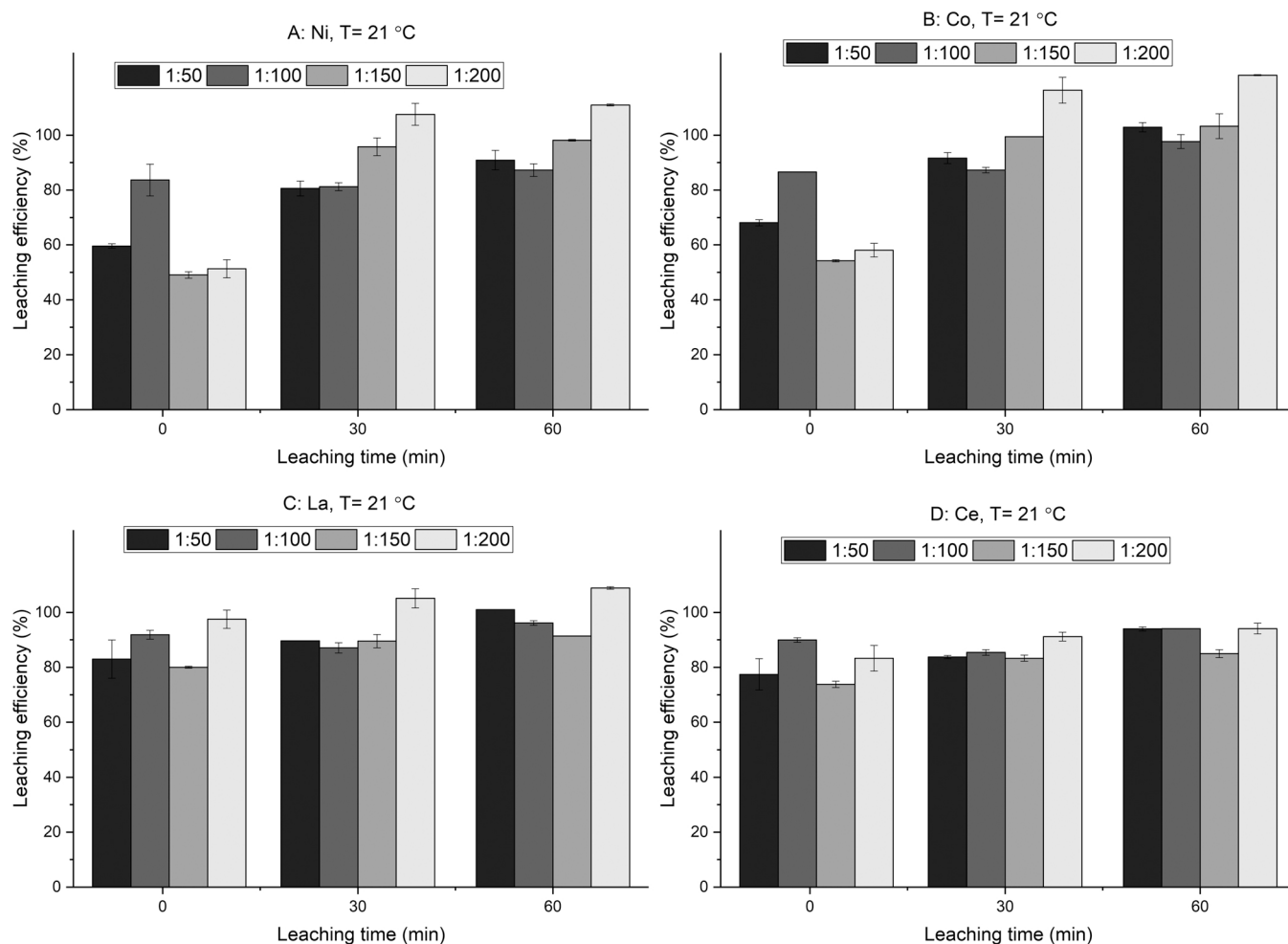


**Fig. 5.** A-D. Effect of S:L-ratio on leaching efficiency (%) of A) Ni, B) Co, C) La, and D) Ce at temperature of 21 °C. Dry chlorination conditions: temperature = 350 °C, residence time = 60 min.

effect of S:L-ratio in the case of REEs, although the most dilute ratio of 1:200 results in the highest yields for La.

By using the generally most economical option of room temperature and an average S:L-ratio of 1:100 with 60 min leaching time, 87% leaching efficiency is reached for Ni, and 94–98% for Co and the REEs. The pH of the leachate was also monitored during the leaching process, and a minor rise in pH from 6.3 to 6.8 during 60 min leaching was observed. The neutral leachate from the water leaching can be considered as an environmentally sounder alternative to acidic leaching solutions. It should be noted that this discovery relies still on the availability of large amounts of water compared to the solid material, and it has been beyond the scope of this paper to consider any recirculation experiments or economic modelling, not to mention separate metal recovery phases downstream or up-scaling. Water consumption could be alleviated by making the leaching step continuous with a parallel metal recovery step through continuous liquid-liquid extraction or ion exchange media. Furthermore, the metal ion concentration in the metal separation and extraction steps is a critical parameter and will need to be evaluated and optimized. In this state after a single leaching step the total dissolved material content is 10 g/l and there is plenty of room to enrich individual metal concentrations if needed by the application. Future studies in this field are currently underway.

#### 4. Conclusions

Dry chlorination of spent NiMH battery waste with  $\text{NH}_4\text{Cl}$  was elucidated to show the effect of dry chlorination and water leaching

parameters on the leaching efficiency of Ni, Co, and the REEs. The amount of NiMH to  $\text{NH}_4\text{Cl}$  was found to have minor effect on the process regards to REEs when 1:1–1:2 wt ratios were used, but Ni and Co required at least a 1:1.5 ratio for sufficient efficiency. A ratio of 1:1.65 was used throughout the work but could be optimized further. Formation of varying reaction products was shown in different dry chlorination temperatures and residence times, with the lower temperatures of 250 and 300 °C resulting in formation of ammonium metal chlorides, of which the ammonium REE chlorides were found to have high solubility in the water leaching. Formation of metal chlorides was only observed in 350 °C after 60 min residence time, where the highest leaching efficiencies for Ni and Co were also reported, indicating better solubility of Ni/Co chlorides compared to ammonium Ni/Co chlorides formed in lower temperatures. Increasing the residence time up to 90 min resulted in generally better leaching efficiencies for the studied metals, after which they remained similar or even decreased. Based on the results, REEs seem to form soluble ammonium REE chloride compounds more quickly and in lower temperatures than Ni and Co. For REEs, excluding lanthanum, a shorter residence time is preferred if the highest temperature of 350 °C is used.

The leaching reaction was found to be rapid for REEs, with 90–94% recoveries immediately after mixing of the sample and water. For Ni and Co, longer leaching times of up to 60 min and the use of higher temperature of 60 °C can be used to reach higher yields in leaching, as well as a more dilute S:L-ratio. For overall highest yields, a temperature of 350 °C and 60 min in dry chlorination followed by room temperature water leaching with an average S:L-ratio of 1:100 and 60 min time



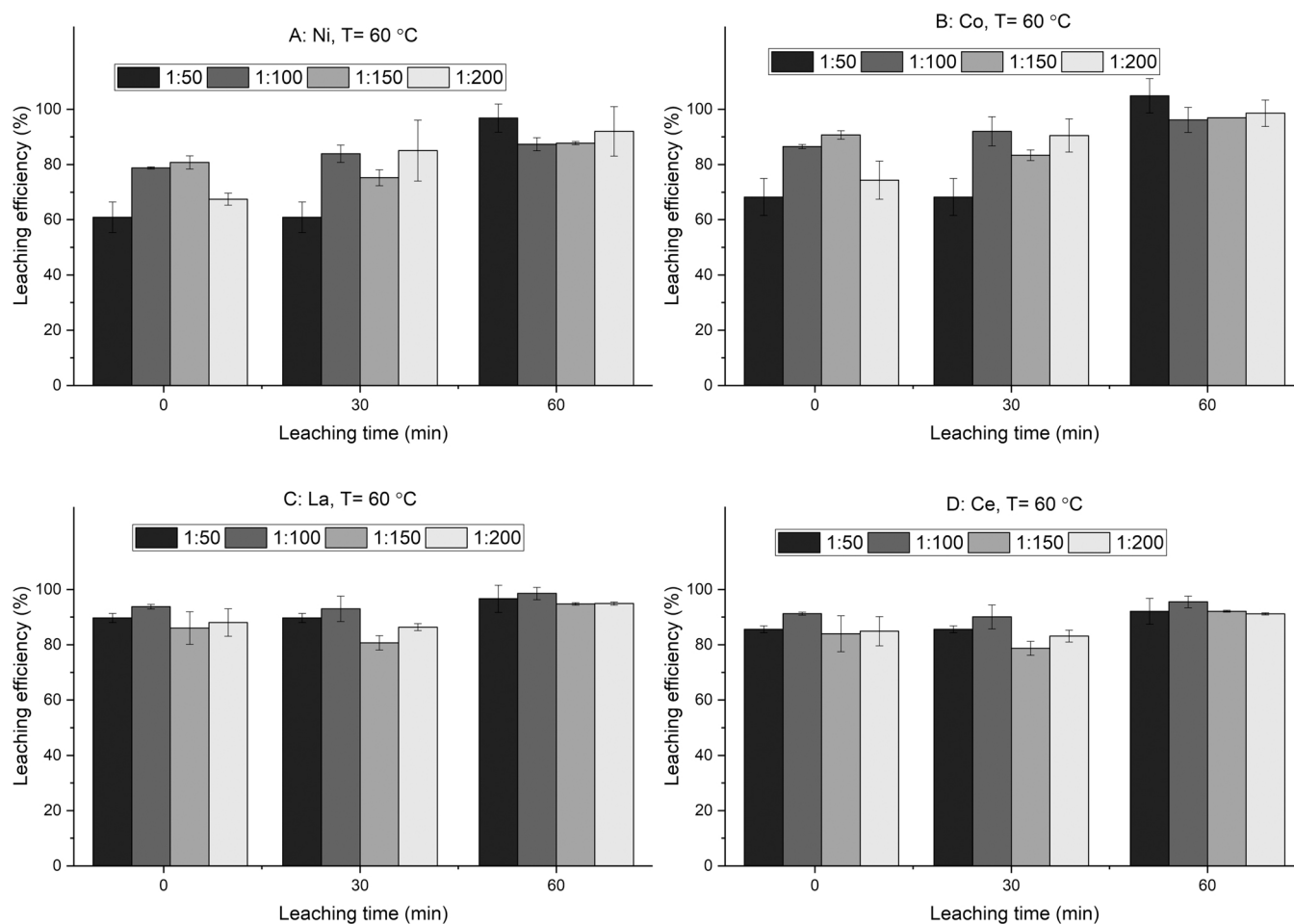


Fig. 6. A-D. Effect of S:L-ratio on leaching efficiency (%) of Ni, Co, La, and Ce at temperature of 60 °C. Dry chlorination conditions: temperature = 350 °C, residence time = 60 min.

results in 87% leaching efficiency for Ni, and > 94% for Co and the REEs. The developed conversion and solubilization process for spent NiMH battery waste is an efficient and environmentally more benign alternative to conventional pyro- or hydrometallurgical processes, where dry chlorination with ammonium chloride in low temperature is employed to produce easily soluble ammonium and chloride containing reaction products. The dry chlorination is followed by simple and efficient water leaching, with neutral leachates and high metal yields, avoiding chemical-intensive neutralization in the following metal separation and recovery stages. Larger scale economics and e.g. water and energy consumption optimization should be studied, but in principle the whole metal recovery pathway could be viable by integrating the process to an existing infrastructure such as a combined heat and power plant environment co-installed with suitable industrial hydrometallurgical process equipment.

#### CRedit authorship contribution statement

**Siiri Perämäki:** Conceptualization, Data curation, Formal analysis, Investigation, Methodology, Validation, Visualization, Writing – original draft, Writing – review & editing. **Antti Tiihonen:** Conceptualization, Data curation; Formal analysis, Investigation, Writing – original draft, Writing – review & editing. **Joona Rajahalme:** Conceptualization, Methodology, Writing – review & editing. **Sylva Larsson:** Data curation, Formal analysis, Investigation, Methodology. **Elmeri Lahtinen:** Conceptualization, Investigation, Methodology, Writing – review & editing. **Joni Niskanen:** Writing – original draft, Writing – review & editing. **Roshan Budhathoki:** Conceptualization, Methodology,

Writing – review & editing. **Ari Väisänen:** Conceptualization, Funding acquisition, Project administration, Resources, Supervision, Writing – review & editing.

#### Declaration of Competing Interest

The authors declare that they have no known competing financial interests or personal relationships that could have appeared to influence the work reported in this paper.

#### Acknowledgements

Dr. Jarmo Louhelainen is gratefully acknowledged for IR-measurements, Hannu Salo for SEM-EDXRF imaging and analysis, and Elina Hautakangas for CHN analysis. Akkuser LTD is appreciated for supplying the spent NiMH battery waste.

#### Funding

This work was supported by the European Regional Development Fund (grant number: A74540) and the Department of Chemistry at University of Jyväskylä.

#### Appendix A. Supporting information

Supplementary data associated with this article can be found in the online version at [doi:10.1016/j.jece.2022.108200](https://doi.org/10.1016/j.jece.2022.108200).

## References

- [1] European Commission, Critical raw materials for the EU, Report of the Ad-hoc Working Group on defining critical raw materials, (2010) 1–84. <https://doi.org/10.1002/eji.200839120>. IL-17-Producing.
- [2] European Commission, Study on the EU's list of Critical Raw Materials (2020) Executive Summary, 2020. <https://doi.org/10.2873/24089>.
- [3] V. Innocenzi, N.M. Ippolito, I. de Michelis, M. Prisciandaro, F. Medici, F. Vegliò, A review of the processes and lab-scale techniques for the treatment of spent rechargeable NiMH batteries, *J. Power Sources* 362 (2017) 202–218, <https://doi.org/10.1016/j.jpowsour.2017.07.034>.
- [4] M. Rinne, H. Elomaa, A. Porvali, M. Lundström, Simulation-based life cycle assessment for hydrometallurgical recycling of mixed LIB and NiMH waste, *Resour., Conserv. Recycl.* 170 (2021), 105586, <https://doi.org/10.1016/j.resconrec.2021.105586>.
- [5] S. Al-Thyabat, T. Nakamura, E. Shibata, A. Iizuka, Adaptation of minerals processing operations for lithium-ion (LiBs) and nickel metal hydride (NiMH) batteries recycling: critical review, *Miner. Eng.* 45 (2013) 4–17, <https://doi.org/10.1016/j.mineng.2012.12.005>.
- [6] T. Müller, B. Friedrich, Development of a recycling process for nickel-metal hydride batteries, *J. Power Sources* 158 (2006) 1498–1509, <https://doi.org/10.1016/j.jpowsour.2005.10.046>.
- [7] J. Lie, J.C. Liu, Selective recovery of rare earth elements (REEs) from spent NiMH batteries by two-stage acid leaching, *J. Environ. Chem. Eng.* 9 (2021), 106084, <https://doi.org/10.1016/j.jece.2021.106084>.
- [8] N.K. Ahn, H.W. Shim, D.W. Kim, B. Swain, Valorization of waste NiMH battery through recovery of critical rare earth metal: a simple recycling process for the circular economy, *Waste Manag.* 104 (2020) 254–261, <https://doi.org/10.1016/j.wasman.2020.01.014>.
- [9] K. Korkmaz, M. Alemrajabi, Å.C. Rasmuson, K.M. Forsberg, Separation of valuable elements from NiMH battery leach liquor via antisolvent precipitation, *Sep. Purif. Technol.* 234 (2020), 115812, <https://doi.org/10.1016/j.seppur.2019.115812>.
- [10] P. Meshram, B.D. Pandey, T.R. Mankhand, Leaching of base metals from spent Ni-metal hydride batteries with emphasis on kinetics and characterization, *Hydrometallurgy* 158 (2015) 172–179, <https://doi.org/10.1016/j.hydromet.2015.10.028>.
- [11] L. Pietrelli, B. Bellomo, D. Fontana, M. Montereali, Characterization and leaching of NiCd and NiMH spent batteries for the recovery of metals, *Waste Manag.* 25 (2005) 221–226, <https://doi.org/10.1016/j.wasman.2004.12.013>.
- [12] M. Ijadi Bajestani, S.M. Mousavi, S.A. Shojasadati, Bioleaching of heavy metals from spent household batteries using *Acidithiobacillus ferrooxidans*: statistical evaluation and optimization, *Sep. Purif. Technol.* 132 (2014) 309–316, <https://doi.org/10.1016/j.seppur.2014.05.023>.
- [13] P. Rasoulnia, R. Barthen, A.-M. Lakaniemi, H. Ali-Löytty, J.A. Puhakka, Low residual dissolved phosphate in spent medium bioleaching enables rapid and enhanced solubilization of rare earth elements from end-of-life NiMH batteries, *Miner. Eng.* 176 (2022), 107361, <https://doi.org/10.1016/j.mineng.2021.107361>.
- [14] X. Su, W. Xie, X. Sun, A sustainable [P6,6,6,14]2[OPBOA]-based separation process of rare earth and transition metal in waste NiMH battery, *Miner. Eng.* 160 (2021), 106641, <https://doi.org/10.1016/j.mineng.2020.106641>.
- [15] A.K. Sahin, D. Voßenkaul, N. Stoltz, S. Stopic, M.N. Saridede, B. Friedrich, Selectivity potential of ionic liquids for metal extraction from slags containing rare earth elements, *Hydrometallurgy* 169 (2017) 59–67, <https://doi.org/10.1016/j.hydromet.2016.12.002>.
- [16] J. Lie, Y.C. Lin, J.C. Liu, Process intensification for valuable metals leaching from spent NiMH batteries, *Chem. Eng. Process. - Process. Intensif.* 167 (2021), 108507, <https://doi.org/10.1016/j.ccep.2021.108507>.
- [17] C.K. Gupta, N. Chrishnamurthy, *Extractive Metallurgy of Rare Earths*, 1st ed., CRC Press, Boca Raton, 2004.
- [18] T. Uda, Recovery of rare earths from magnet sludge by FeCl<sub>2</sub>, *Mater. Trans.* 43 (2002) 55–62, <https://doi.org/10.2320/matertrans.43.55>.
- [19] M. Itoh, K. Miura, K. Machida, Novel rare earth recovery process on Nd-Fe-B magnet scrap by selective chlorination using NH<sub>4</sub>Cl, *J. Alloys Compd.* 477 (2009) 484–487, <https://doi.org/10.1016/j.jallcom.2008.10.036>.
- [20] T. Lorenz, M. Bertau, Recycling of rare earth elements from FeNdB-Magnets via solid-state chlorination, *J. Clean. Prod.* 215 (2019) 131–143, <https://doi.org/10.1016/j.jclepro.2019.01.051>.
- [21] G. Micco, F. Pomiro, J. Grau, A. Bohe, Zinc recovery from spent chemical sorbent by dry chlorination and electrodeposition from chloride solutions, *Int. Res. J. Pure Appl. Chem.* 14 (2017) 1–13, <https://doi.org/10.9734/irjpac/2017/35288>.
- [22] T. Kuzuya, S. Hirai, V. Sokolov, Recovery of valuable metals from a spent nickel-metal hydride battery: Selective chlorination roasting of an anodic active material with CCl<sub>4</sub> gas, *Sep. Purif. Technol.* 118 (2013) 823–827, <https://doi.org/10.1016/j.seppur.2013.08.008>.
- [23] M. Kaya, *Electronic Waste and Printed Circuit Board Recycling Technologies*. First Edit, Springer, Switzerland, 2019, <https://doi.org/10.1007/978-3-030-26593-9>.
- [24] J. Zhang, B. Zhao, B. Schreiner, *Separation Hydrometallurgy of Rare Earths Elements*. First Edit, Springer, 2016, <https://doi.org/10.1007/978-3-319-28235-0>.
- [25] E. Ma, Chapter 11 – Recovery of Waste Printed Circuit Boards Through Pyrometallurgy, in: M.N. v. Prasad, M. Vithanage (Eds.), *Electronic Waste Management and Treatment Technology*, First Edit, Butterworth-Heinemann, 2019: pp. 247–267.
- [26] Y. Ma, X. Zhou, J. Tang, X. Liu, H. Gan, J. Yang, One-step selective recovery and cyclic utilization of valuable metals from spent lithium-ion batteries via low-temperature chlorination pyrolysis, *Resour., Conserv. Recycl.* 175 (2021), 105840, <https://doi.org/10.1016/j.resconrec.2021.105840>.
- [27] W.M. Haynes, D.R. Lide, T.J. Bruno (Eds.), *CRC Handbook of Chemistry and Physics*, 97th ed., CRC Press, Taylor and Francis Group, Boca Raton, 2017.
- [28] T. Lorenz, K. Golon, P. Fröhlich, M. Bertau, Recycling of rare earths from Hg-containing fluorescent lamp scraps by solid state chlorination, *Chem. Ing. Tech.* 87 (2015) 1373–1382, <https://doi.org/10.1002/cite.201400181>.
- [29] T. Lorenz, P. Fröhlich, M. Bertau, Rückgewinnung seltener erden aus FeNdB-Dauermagneten mittels Feststoffchlorierung, *Chem. Ing. Tech.* 89 (2017) 1210–1219, <https://doi.org/10.1002/cite.201600171>.